Lessons Learned from Recent Space Flight Assessments

James P. Smith[1], Kenneth R. Hamm Jr[2]. Kauser S. Imtiaz[3] and Ivatury S. Raju[4]
NASA Langley Research Center, Hampton, Virginia

ABSTRACT

This paper highlights four space flight assessments, each with an important lesson. The first assessment points to the challenge of material substitution for weight saving. Space Shuttle's external tank stringers were changed from Al 2024 to Al 2090 without comprehensive analysis. Lack of understanding the low Short-Transverse (S-T) strength associated with Al 2090 led to widespread cracking. The second assessment addresses the failure to understand that time-dependent relationships and loading interactions of multiple disciplines can lead to non-conservative results. An aerodynamic test article of the Orion Multi-Purpose Crew Vehicle (MPCV) Launch Abort System (LAS) was analyzed for worst-case single discipline loads, showing positive structural margins. When disciplines were combined with time dependent loading, the analysis resulted in negative margins. The third assessment highlights the pitfalls of putting blind trust in historical architecture. The MPCV re-entry heat shield adopted the Apollo design approach despite fundamental differences between the two designs (e.g., the underlying substructure design, material differences, scale, and geometry). Manufacturing resulted in cracking along seams of the cured MPCV heat shield and produced lower mechanical properties of the Avcoat witness panels. Subsequently, the design was changed to a block architecture, which introduced unperceived technical, cost, and schedule risk. The fourth assessment shows how the lack of a comprehensive investigation of design modifications and inappropriate Finite Element Analyses (FEA) can lead to trouble. A mass reduction campaign eliminated highly critical internal struts on the ISS Node-1 pressurized module based on inadequate and uncorrelated FEA. High strains were noted and ignored as a modeling aberration. A system level high fidelity FEA discovered large plastic strains in the gussets of all four radial ports. These findings initiated a full-scale test campaign, new test correlated assembly-level FEA, and significant design modifications.

---

[1] Senior Engineer, NASA Johnson Space Center, Houston, TX

[2] NESC Chief Engineer at Ames, Senior Member AIAA, Member ASME, NASA Ames Research Center, Mountain View, CA

[3] NASA Technical Fellow for Structures, Associate Fellow AIAA, Senior member ASME, NASA Johnson Space Center, Houston, TX

[4] Distinguished Research Associate, Durability, Damage Tolerance, and Reliability Branch, Fellow AIAA, Fellow ASME, Member ASCE.

INTRODUCTION

The true nature of the successes and shortcomings of a space flight becomes apparent as the flight design matures only after test flights, or as a result of operational failures or loss of mission. Assessments and analyses of each flight are of utmost importance as failures, mishaps, missteps, and shortcomings reveal lessons to be learned. Success of subsequent flights depends on not repeating these errors, mistakes, missteps, and poor decisions. Such learning lessons should be a top priority for space flight programs. To avoid repeating mistakes, engineers must pay attention to historic events and make sure the valuable lessons are recorded, learned, and assimilated. This paper presents lessons learned from four recent space flight assessments and highlights some of the shortcomings observed in thought processes, hardware configurations, analyses, and experimental methods.

Those who cannot learn from history are doomed to repeat it.

– George Santayana

Lesson Learned 1: 'Inconsequential' Design Changes Seldom Are:

The Space Shuttle External Tank (ET) consists of liquid hydrogen (LH2) tank, liquid oxygen (LOX) tank, and intertank (IT). LH2 and LOX propellants were the fuels for the Orbiter's three main engines. The ET also served as the structural backbone of the Space Transportation System (STS), providing for attachment of the Orbiter and the Solid Rocket Boosters (SRBs).

On November 5, 2010, the launch of Space Shuttle mission STS-133 was scrubbed after propellant loading, due to a gaseous hydrogen leak at the ground umbilical connection to the ET. During visual inspections following the scrub, an anomalous crack in the ET sprayed-on foam insulation (SOFI) was observed at the forward end of the IT near the interface of the LOX tank (Figure 1). Removal of the damaged foam revealed that an underlying aluminum hat-section stringer had cracked approximately 9 inches along each side, just inboard of the fasteners that attached the stringer "feet" to the IT forward flange chord[1-3] (Figures 1 and 2).

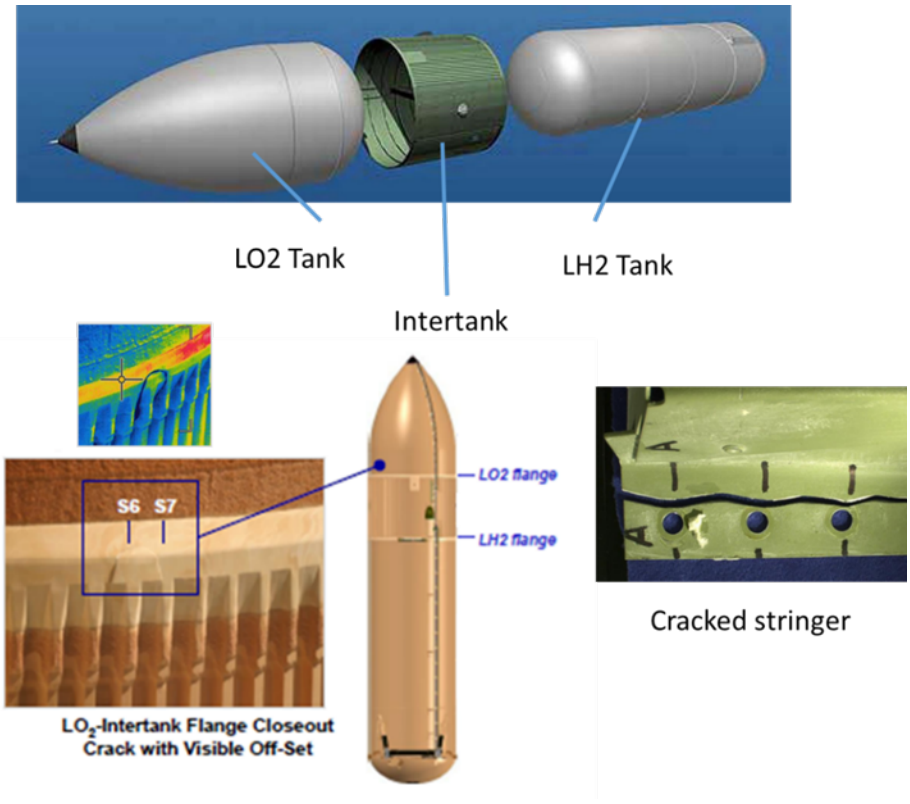

Figure 1. External Tank and Cracking near LO2 Tank-Intertank Interface

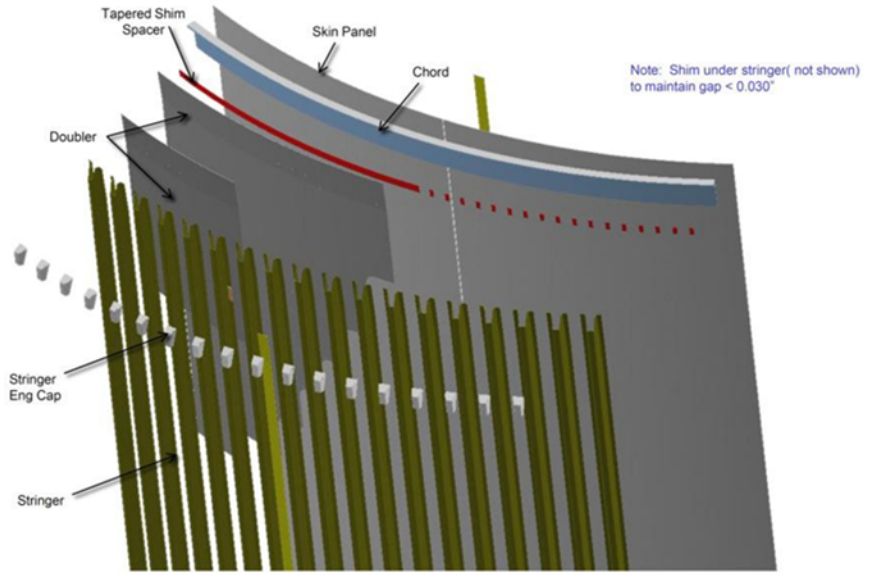

Figure 2. Representative IT panel with external hat stringers

Closer inspection of this region revealed that two hat-shaped stringers, Panel 2 - Stringers 6 and 7, had through-cracks along the stringer feet between the fasteners and the stringer sidewall. These two IT stringers were repaired at the launch pad, and a second tanking of ET-137 was performed with considerable added instrumentation which showed additional anomalies in the IT region. The vehicle was returned to the Vehicle Assembly Building (VAB) and a full 360-degree inspection was conducted. This inspection revealed three additional stringer cracks (Panel 6 - Stringers 6, 7 and 11). These stringers were repaired, and the vehicle was then rolled back to the launch pad. Various material and structural investigations and assessments were initiated to understand the root cause of the IT stringer cracking, to develop and assess repair options, and to develop flight rationale for STS-133.

The IT is an unpressurized, stiffened cylindrical structure that serves as the structural connection between the liquid propellant tanks. The IT also functions to receive and distribute all thrust loads from the SRBs. An assembly of eight curved panels are mechanically joined into a barrel with five internal ring frames to form the IT. Of the eight panels, two diametrically opposite panels are connected to the SRB box beam. The box beam reacts the majority of the SRB thrust loads. These two panels are thick plate, one piece panels, with integrally machined blade stiffeners and pocketed membrane areas[3]. The other six IT panels are manufactured from sheet metal skins with externally mounted, hat-section stringer stiffeners. These stringers are mechanically attached with rivets along most of their length and with specialty fasteners, such as GP Lockbolts and Hi-Loks, at the forward and aft ends where the stringers attach to flange chords. The hat-section stringers are fabricated from aluminum sheet using a combination of rolling and hot-forming processes. There are 18 stringers per panel, located on approximately 7-inch centers[1-3].

Over the history of the Space Shuttle Program, there were been two major revisions of the ET design to decrease structural weight. The general structural configuration of the IT remained unchanged throughout those changes. The last major evolution from Lightweight Tank (LWT) to the Super Lightweight Tank (SLWT) involved a widespread change of skin/stringer material from aluminum alloy Al-2024 to aluminum-lithium alloy Al-2090[2] to reduce mass.

The basic assumption made regarding the November 5th IT stringer cracking event, was that a rogue IT stringer existed, and after the ET tanking event, the strain in the stringer feet due to tanking alone was just below the failure strain. This premise led to the conclusion that a relatively high combined assembly and tanking strain level existed in the stringer feet between the fastener and the stringer sidewall. However, investigation determined the magnitude of the assembly strain not to be additive to the strain resulting from the operational loading events.

To better understand these effects and assess the influence of plasticity, elastic-plastic, large-deflection nonlinear thermomechanical stress analyses were performed for the IT external hat-shaped stringers[1]. Detailed 3D FE models were developed and analyzed to investigate the elastic-plastic response of the IT stringers and to assess the potential for local failure to develop in the stringer feet. The stringers were subject to assembly strains caused by initial installation on an IT panel. Transient thermal loading occurred in these stringers as the LOX tank was filled prior to launch. Other bounding mechanical loading events were present for pre-tanking, pre-launch, and flight-loading events. These extensive analytical and experimental investigations concluded that

these stringers failed due to the material short-transverse capability being less than and the stresses being greater than expected. Material studies documented that, "Alloy 2090 rolled products are known to have dramatically reduced material properties in specific directions relative to the rolling direction, especially in thin-sheet material. Short transverse and longitudinal (long transverse) properties are important for the initial stages of stringer crack propagation and for later stages of through-the-thickness cracking, repesctively"[4]. The greater than expected stresses were attributed to unexpectedly higher assembly-induced stresses that combined with stresses resulting from cryogenically induced deflections.

All five stringers in which cracks were found were repaired. The remaining Al-2090 stringers were reinforced with radius blocks at the LOX tank end of the stringers (see Figure 3). The SOFI at the LOX tank interface was removed prior to the mechanical installation of the radius blocks, and after all radius blocks were installed, the insulation was reapplied and trimmed to flight configuration. Significant analysis and test efforts concluded that the radius blocks were effective in restoring the structural capability and that they had no detrimental system level side effects.

The cracking did not occur on the previous flights as the original Al-2024 was a ductile material with homogeneous and near isotropic properties. In contrast, the Al-2090 was an orthotropic material with reduced material properties in specific directions (i.e., Short-Transverse, S-T). Documentation showed Material and Processing (M&P) engineers had previously warned against the use of this material in regions of large stresses but that message was lost/ignored over time.

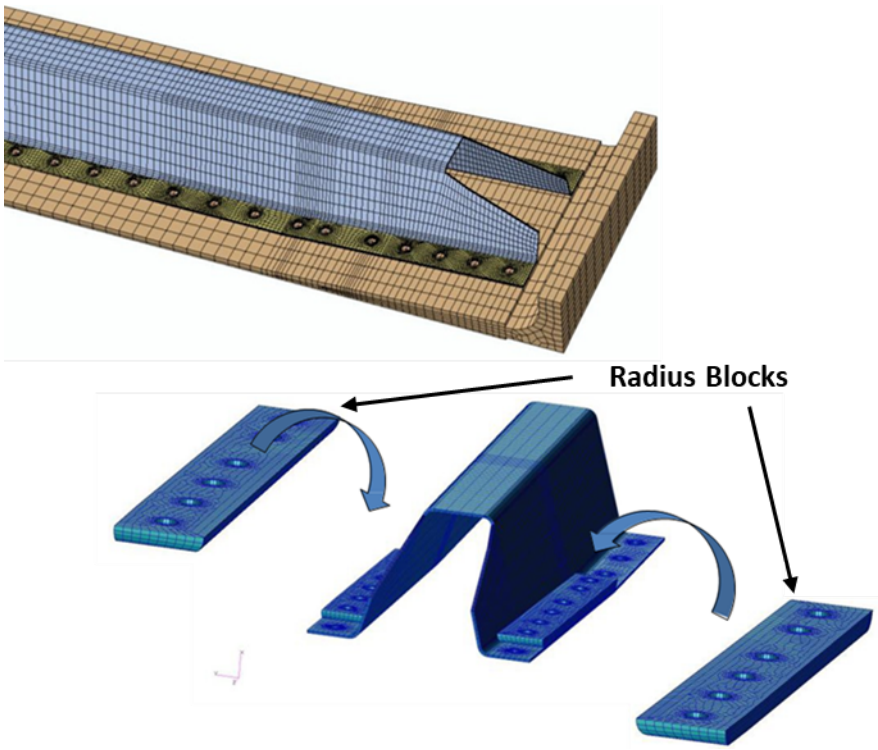

Figure 3. Hat stringer and radius blocks

Lessons: 1) Listen to discipline experts and follow their advice. 2) Avoid making material substitutions without a comprehensive study of all aspects of the hardware configuration and loadings.

Lesson Learned #2: Worst on Worst Is Not Always Worse:

In recent years, advanced multi-physics/multi-disciplinary analysis techniques and tools have become more widely used in the areas of structural design for aerospace vehicles. Advanced software packages now possess the ability to account for differing physical behaviors simultaneously within a simulation run. These methods usually come at a cost of increased model complexity, longer run times, and may require the inclusion of time dependent behavior in the analysis. Often advanced analysis, if performed, does not occur until after the designs have been partially developed and, in some cases, after the design is finalized and manufacturing has started. Results from these higher fidelity analyses may uncover design defects that were unanticipated or unaccounted for in the preliminary design/analysis process where traditional methods, using modified properties (i.e., material knockdowns) and/or simplified assumptions are the norm. It is vitally important for hardware design/analysis cycles to account correctly for multi-discipline environmental effects early in their development to reduce the possibility of significant design changes being required late in the process, when they tend to be much more expensive to correct.

An example of this type of issue occurred during the development and testing for aeroacoustic environments on the ORION/Multi-Purpose Crew Vehicle (MPCV) Launch Abort System (LAS). This testing, known as the 80-AS test series, was performed at Ames Research Center in 2009-2010. Panda et al.[5] provides details of the goals, procedures, and results of that testing.

The ORION/MPCV LAS system consists of an aerodynamic fairing assembly that protects the spacecraft from external aerodynamic and aeroacoustic loading during launch and ascent or abort. In the event of an abort, a set of solid rocket motors fire to pull the ORION Crew Module (CM) and crew away from the Space Launch System (SLS) stack. Control motors also provide attitude control. Figure 4 shows an illustration of the ORION/MPCV LAS.

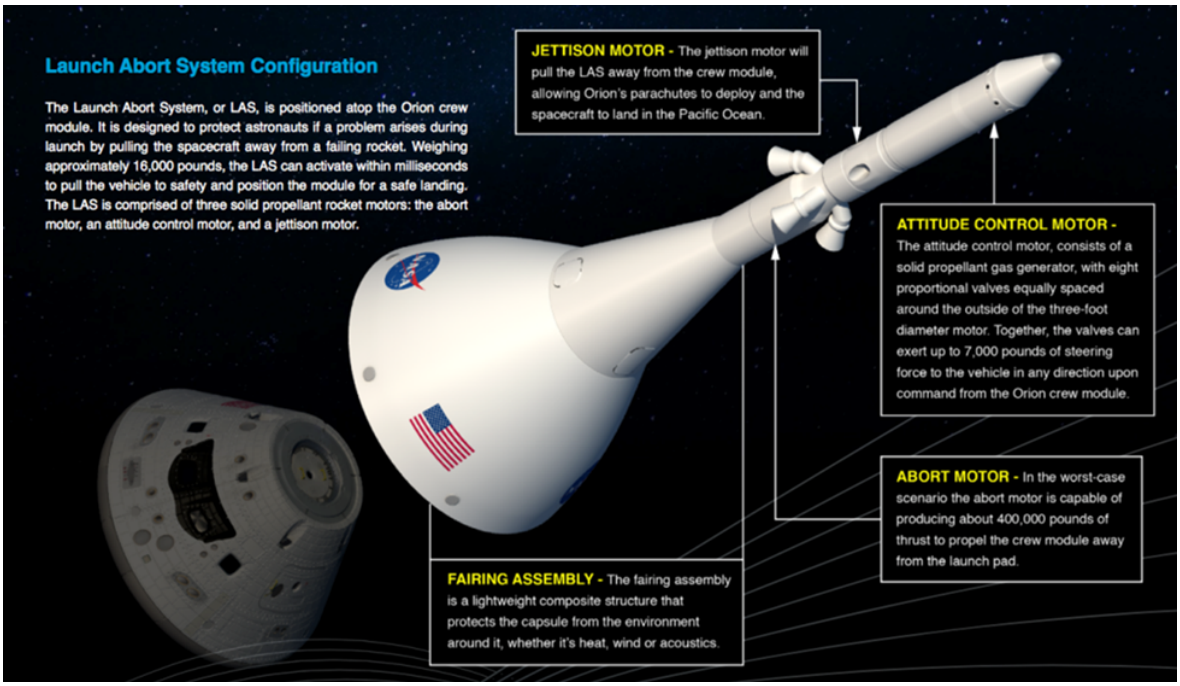

Figure 4. ORION Launch Abort System[6]

Thrust impingement and high acoustic loads produced by abort rocket motor exhaust onto the LAS fairing assembly during a launch abort were known design issues. The ORION program decided to conduct simulations and measurements of this acoustic environment by means of wind tunnel testing. This testing was performed in the 11-Foot Transonic Wind Tunnel facility at the Ames Research Center using a LAS model with simulated abort motor exhausts. A scale model of the LAS, shown in Figure 5, was developed to measure the magnitude of these acoustic loads in different flight regimes. This scale model included internal ducting for the routing of hot helium gas through the model allowing it to exit at the abort motor nozzle locations and impinge directly onto the fairing. Helium was selected due to the similarity of acoustic energy transmission properties at elevated temperature, compared to the actual abort motor exhaust. Tunnel airflow around the exterior of the model provided simulation of transonic aerodynamic pressures and flow effects.

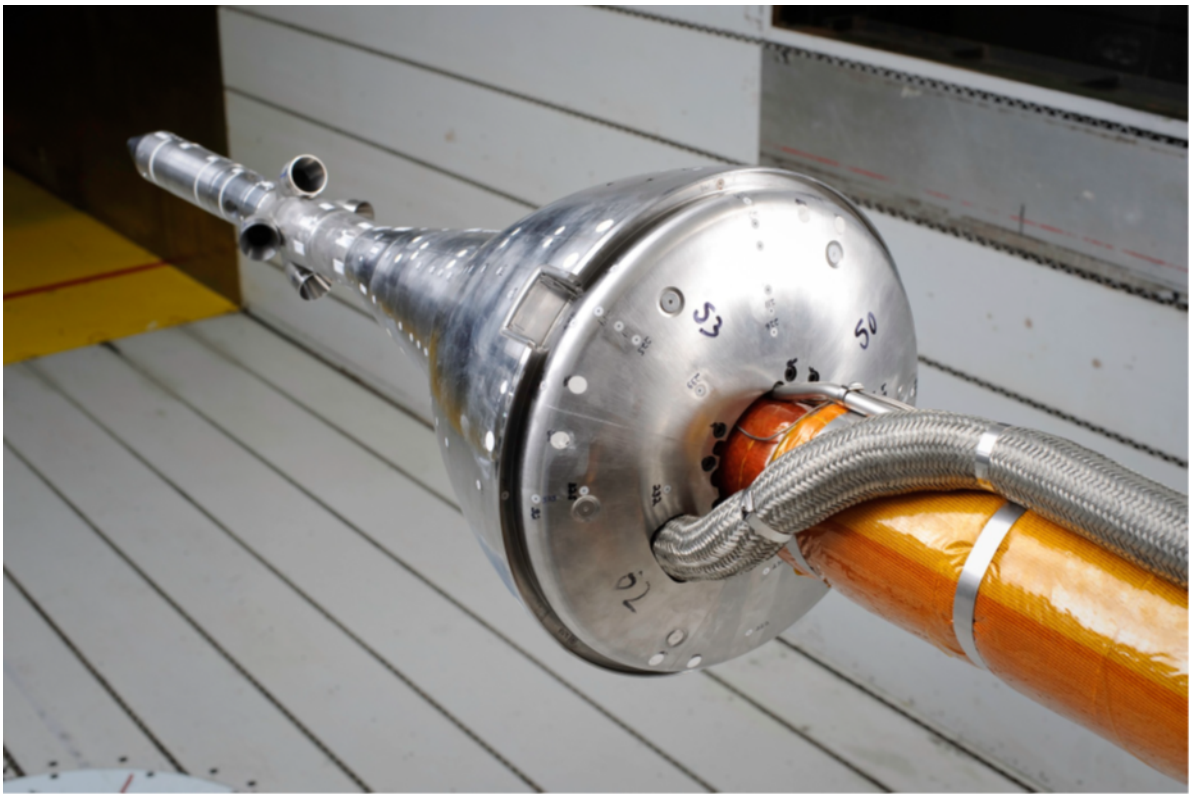

Figure 5. 80-AS Test Article Installed in ARC Transonic Wind Tunnel

The test article preliminary design used linear static analysis, performed in Parametric Technology Corp. (PTC) Pro-Mechanica, and accounted for the loads due to transonic airflow and pressure imparted by tunnel conditions. Steady state pressures, obtained from CFD flow simulation of various tunnel test conditions, were applied to the structural finite element model and were believed to account for worst-case structural loading and stresses.

Elevated temperature effects on the structure were accounted for in the following manner. Temperatures obtained from steady state thermal analyses, performed via a Thermal Desktop simulation, allowed determination of strength property knockdowns, using graphs of material temperature dependency from MMPDS[7], for the various materials used in fabrication. In this way, strength margins were determined using the stress values obtained via static analysis of pressure loads only, which were compared with reduced allowable strengths, based on the steady state temperature analysis of the test article. Differential thermal strain effects were not considered, and believed to be minimal at worst-case steady-state temperature conditions predicted by analysis.

The wind tunnel model design used precipitation hardened (PH) stainless steel, incorporating different heat treatments of 17-4 PH with differing CTE values over the temperature range. The nozzle assembly, representing the locations of the abort rocket motors, was fabricated from a chrome-based material to resist heat loading, also with differing CTE. Differing elastic moduli and CTE values at various temperature are outlined in Table 1.

Table 1: Mechanical and Thermal Properties at RT and Elevated Temp (MMPDS-04)

Material	E @ 70ºF ($x10^6$ psi)	E @800ºF ($x10^6$ psi)	CTE @70ºF ($x10^{-6}$ in/in/ºF)	CTE @ 800ºF ($x10^{-6}$ in/in/ºF)	Density (lb./in^2)
CoCr (Nozzle)	30.5	30.5	7.5	7.5	0.322
17-4 PH (H900)	28.5	23.37	5.8	6.5	0.282
17-4 PH (H1075)	28.5	23.37	6.2	6.8	0.283
17-4 PH (H1150)	28.5	23.37	6.2	7.2	0.284

Results from the preliminary sets of analyses showed positive margins for all parts based on the loading and stresses resulting from these steady state assumptions. Therefore, in order to meet schedule constraints for wind tunnel test times, the design was released for fabrication of components before final design reviews were completed.

In actuality, the test simulation environment was highly transient. As shown in Figure 6, as the test progressed, flow of the hot gas cycled on and off through numerous cycles over about thirty minutes (2010 seconds). In periods when hot gas was not flowing, the test article structure was effectively cooled by the tunnel airflow over the model exterior, and by room-temperature air flowing through the interior ducting and discharging through the nozzles. The model gradually heated up from the inside following these cycles. Over the first several cycles, exterior parts exposed to the tunnel airflow did not heat, but interior surfaces heated much more quickly. Differential thermal strain developed between structural parts and contributed significantly to the stress.

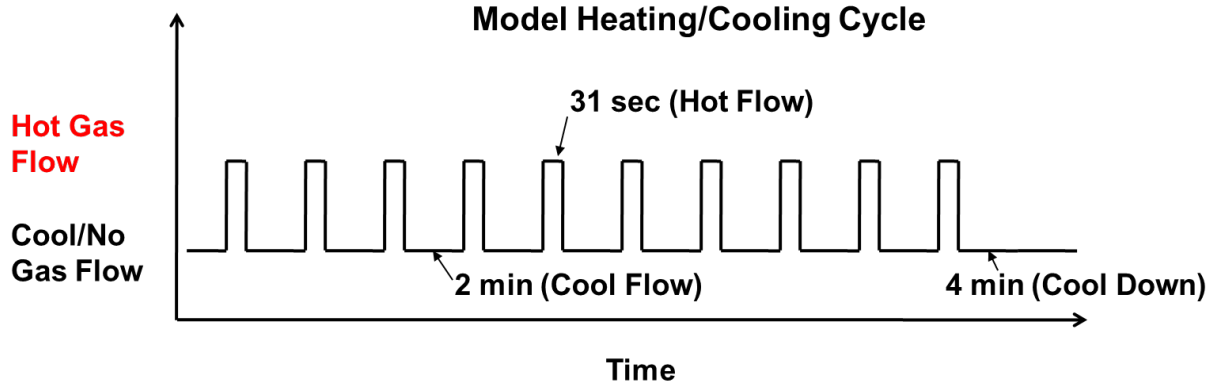

Figure 6. Gas Thermal Cycles

To ascertain if thermal transient response would be a safety issue, a new finite element model was constructed in MSC-NASTRAN to simulate the thermo-structural transient effects. A solid model composed of mostly CHEXA elements was used to predict both the transient temperatures and the thermo-structural stress results. Using the same mesh for both analyses allowed for easy transfer of nodal temperatures without a complicated mapping or interpolation of temperature data between dissimilar meshes. Details of the various components of this model are shown in Figure 7.

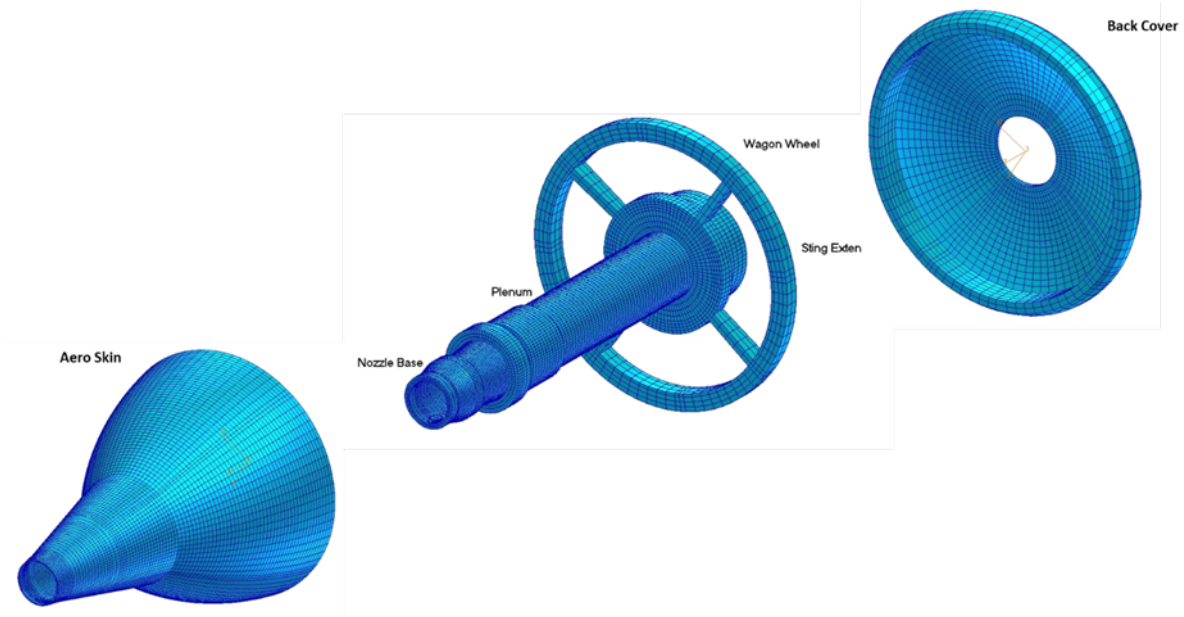

Figure 7. FE Mesh for Thermo-Structural Analyses

The first part of this new analysis sought to predict transient temperature throughout the test article structure over the entire thirty minutes of simulation. MSC-NASTRAN solution 159 (Transient Thermal) was used to generate a temperature profile at each second of the 2010-second tunnel test run. Convection boundary conditions were applied to the interior plenum surfaces exposed to the flow of hot and cold gas flow, and the exterior model surfaces exposed to both tunnel flow and the simulated exhaust plumes. Material conduction properties were applied to the solid portions of the model and contact resistance between mating parts was simulated with 1-D thermal contact elements. The results of this simulation showed significant thermal gradients in the structure, especially in the first few heating cycles as illustrated in the three plots of Figure 8.

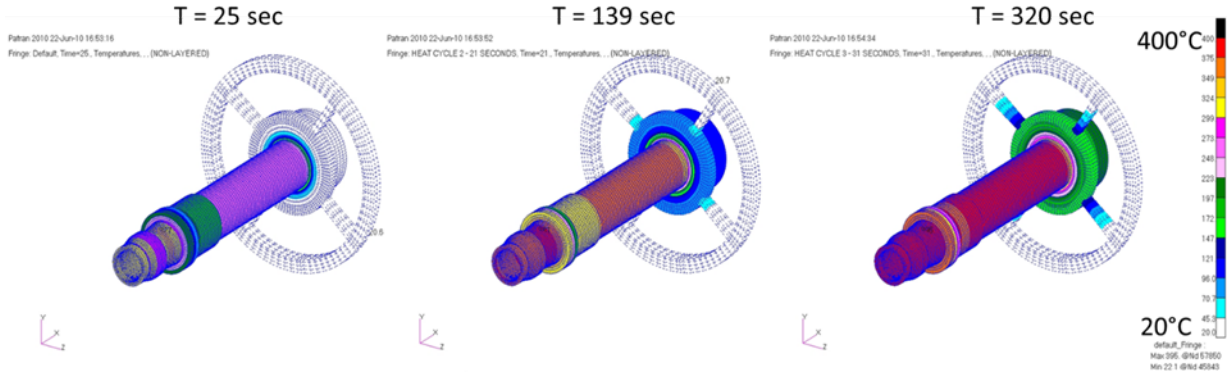

Figure 8. Temperature Distribution in Interior Components at Three Time Steps

Transient temperatures saved from each time step were used as temperature loading inputs for MSC-NASTRAN linear static analyses (Sol 101). Material property temperature dependency was accounted for in the material definitions. Structural effects of the transient thermal gradients were

combined directly with the external and internal pressure loading to give an overall thermo-structural response of the model hardware for each second of the simulation.

The simulation now allowed the model to gradually heat from the inside, following the heating/cooling cycles. Thermal strain now developed between structural parts. These more accurate results showed an increase in loads and stresses in the components of the test article, especially at joints, due to pressure effects combined with transient flow of heat. Stress levels were significantly higher in the first 3-4 transient cycles than had been predicted by steady state analyses, as is shown in Figure 9 and Table 2[8]. Figure 9 illustrates the peaking of stress in the early heating/cooling cycles resulting from thermal transient behavior.

Table 2. Von Mises Stress in Structural Components of 80-AS Model

Time (sec)	Nozzle Stress (ksi)	Plenum Stress (ksi)	Sting Stress (ksi)	Skin Stress (ksi)	Wagon Wheel Stress (ksi)	Back Cover Stress (ksi)
0.0	44.6	35.1	12.0	4.6	4.7	5.1
1.0	44.2	34.5	17.2	4.2	6.1	6.2
25.0	44.9	74.5	**77.3**	**53.0**	66.1	71.6
139.0	46.3	**82.6**	62.5	49.8	83.4	96.8
320.0	**47.0**	71.1	46.3	45.4	**85.4**	**103.4**
581.0	46.9	57.0	33.6	37.5	78.0	96.8
737.0	47.0	51.6	27.4	37.0	76.6	95.6
913.0	46.9	47.1	26.3	36.5	74.5	93.0
1131.0	47.0	43.7	25.3	36.2	72.8	90.0
1338.0	46.9	41.2	24.7	36.1	71.7	88.2
1557.0	46.9	40.4	24.2	36.0	70.5	86.4
1779.0	46.9	39.5	23.8	36.0	69.4	84.9
2010.0	46.8	38.9	23.4	36.1	68.3	83.6

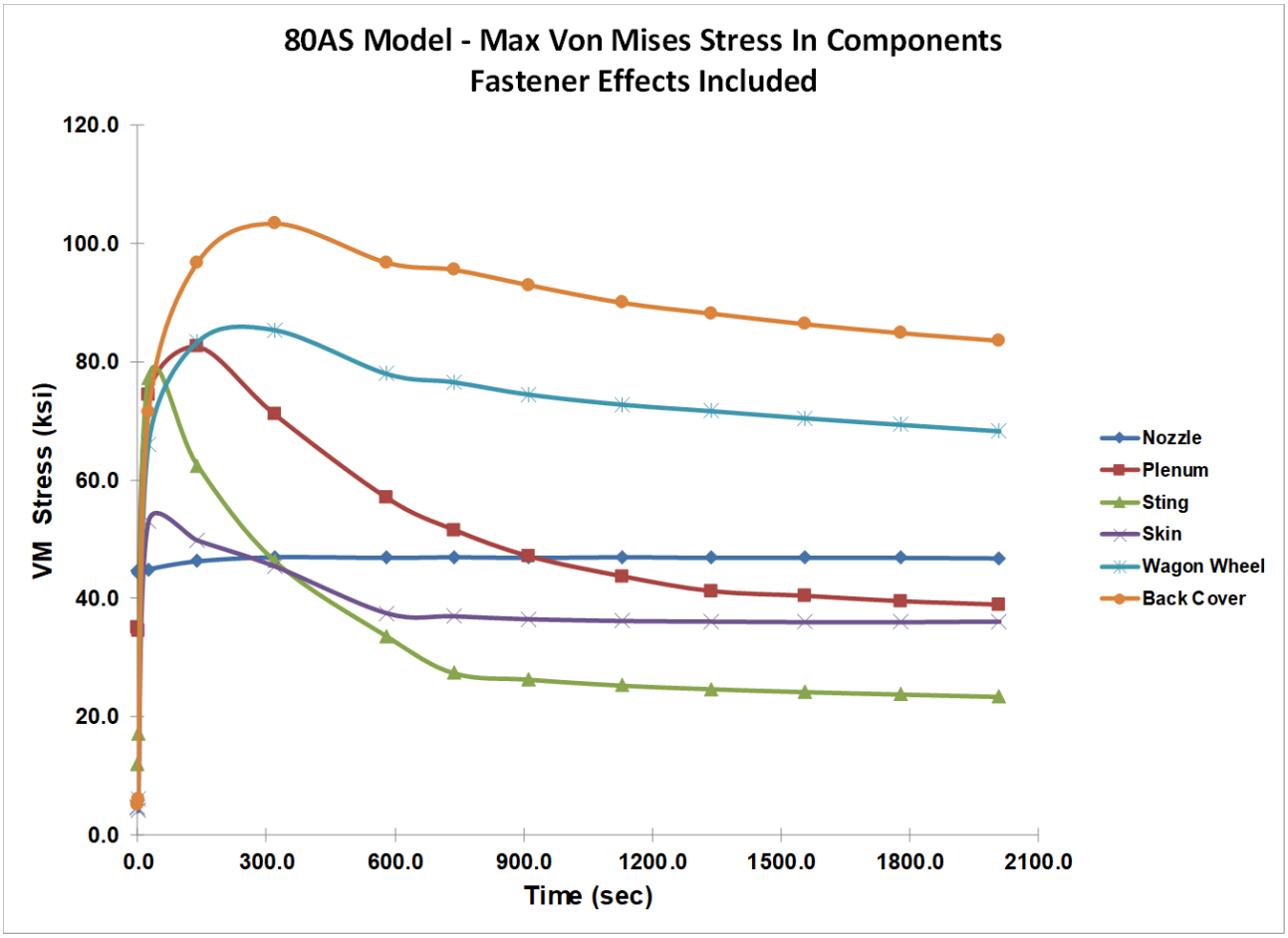

Figure 9. Stress Effects Resulting from Thermal Transients

Margins, which originally had shown positive, were now negative in many locations. However, much of the hardware was already fabricated - a result of starting manufacturing based on the results of the earlier steady state analysis. Test schedules in the ARC wind tunnel were set and did not allow sufficient time for hardware re-design or re-manufacture.

Based on results from the more detailed transient analysis, a plan was developed to perform detailed inspection of the test article throughout the test campaign after each data collection run. Locations of predicted high stress and negative margin were identified and an inspection plan was developed to check for onset of fatigue failure or overload in any components or fasteners. Using this analysis-based inspection process, the entire test series was completed successfully, without incident, and vital data for ORION LAS design was obtained.

This example demonstrates the need for engineers to be aware of how loading is applied and the need to capture its character and effects correctly. Loading from different disciplines, in this case thermal and mechanical acting together and affecting each other, must be accounted for properly. These interactions can be vital in understanding true behavior of a complex structure. The original analysis attempted to capture the thermal and mechanical aspects of the environment by using a

worst on worst assumption, but failed to understand how their time dependent relationship might affect the analysis result.

> *Lesson: Understanding the appropriate simulation of time-dependent environments in structural analysis is of utmost importance. Preconceived assumptions of how environments may or may not interact may produce inaccurate or non-conservative results.*

Lesson Learned #3: Heritage Does Not Mean It Works As It Did Previously:

A lesson that continues to be learned is the two-edged sword of both placing blind trust into historical architectures and the "grass is greener" syndrome. An example of this is the changing architecture of the NASA Orion Multi-Purpose Crew Vehicle (MPCV) re-entry heat shield. NASA's experience with the Apollo Program architecture[9] was the basis for the Orion heat shield design. That design entailed the bonding of a fiberglass and phenolic honeycomb onto a structural substrate followed by the manual injection of Avcoat 5026-39 into the individual cells of the honeycomb. This laborious process, shown being performed in Figure 10, introduces unique workmanship issues such as variability of technique of the numerous technicians responsible for the Apollo heat shield fabrication. For example, the speed and pressure applied during the injection process as well as the angle at which the tool is held can introduce process variability.

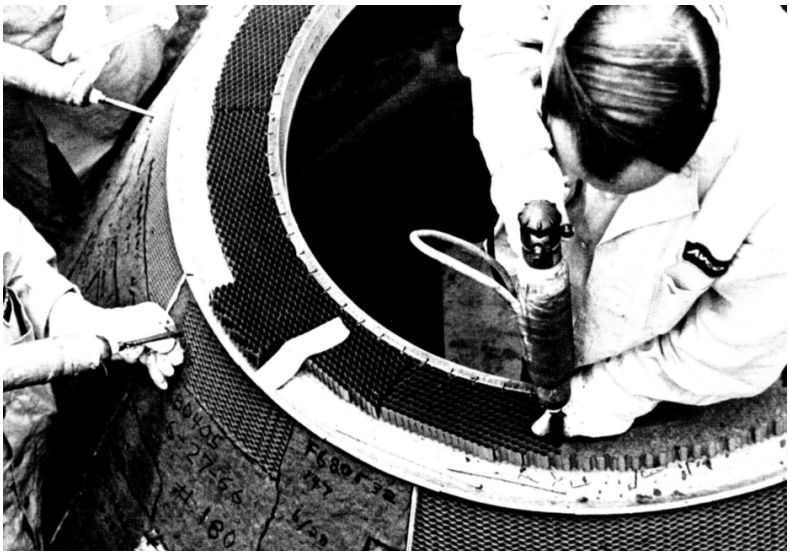

Figure 10. Manual injection of Avcoat 5026-39 into Apollo heat shield honeycomb[9]

By comparison, some five decades later, the heat shield fabrication on the Orion MPCV followed many of the same processes. The manual injection process, shown in Figure 11, was largely unchanged. This manual process involved injecting over 300,000 individual cells by hand to create a rough form of the ablative heat shield followed by non-destructive evaluation using X-ray.

Afterwards, the rough surface was machined down to a smooth, final flight profile per the drawing specifications.

Figure 11. Manual injection process implemented on Orion EFT-1 heat shield
(https://www.nasa.gov/content/partnerships-make-missions-possible)

However, even though the touch labor processes for these two heat shield designs, decades apart, were similar, fundamental differences existed between the heritage Apollo design and the Orion implementation, including:

- Apollo used a stainless steel plate and honeycomb substructure[9] whereas Orion used a composite substructure with a titanium backbone[10] (Figure 12)
- Material constituents used in the Apollo era Avcoat mixture were no longer available in the Orion era due to modern environmental regulations
- Differences in how requirements were levied, such as the use of average material properties during Apollo and A-basis properties for Orion and how design factors were levied on the thermally induced loads
- Apollo's heat shield diameter was 154 inches compared to Orion's diameter of 198 inches[10]

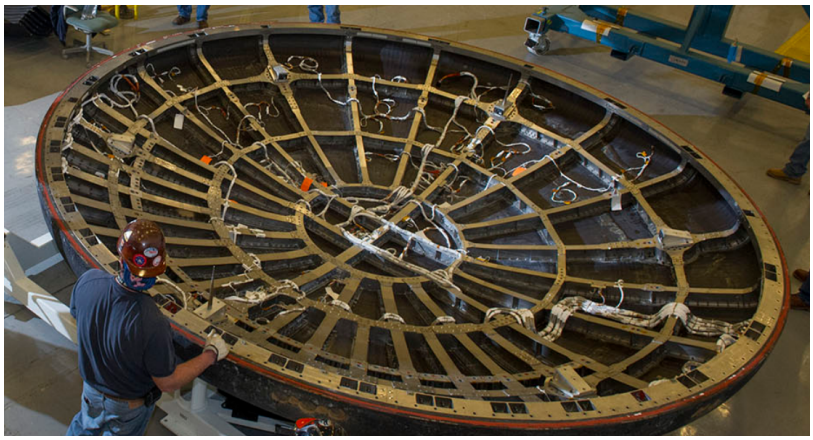

Figure 12. Orion Heatshield Substructure
(https://www.nasa.gov/centers/marshall/news/news/releases/2015/heat-shield-for-nasas-orion-continues-post-flight-journey-by-land.html)

The difference in structural design has certain implications for the thermo-mechanical response of the heat shield system. The mechanical stiffness of the Apollo steel sheet and honeycomb design is significantly different from Orion's quasi-isotropic composite laminate and titanium backbone system. The Apollo system provides for repeatable mechanical response (i.e., essentially isotropic-like bending response), but the circumferentially and radially stiffened Orion system allows for local bending between stiffeners.

The combined system coefficients of thermal expansion between the Orion and Apollo architectures differ greatly due to the materials selected as the backbone and substrate. The thermal properties of the architectures are just as varied as the mechanical properties, with drastically different thermal conductivities, specific heats, and mass densities. Despite these fundamental differences, the Avcoat ablative solution derived from Apollo was applied to the new Orion spacecraft.

During manufacturing, two significant issues were uncovered[10], namely the presence of cracking along some seams in the cured heat shield and Avcoat witness panels that were found to have lower mechanical strength than the specimens used in the population for development of material strength design allowables. An example of fabrication induced cracking is shown in Figure 13 for two locations on the heat shield. The image on the left shows locations of the cracks, most of which are aligned with the radial coordinate direction and are located in the unsupported regions between radial stiffeners.

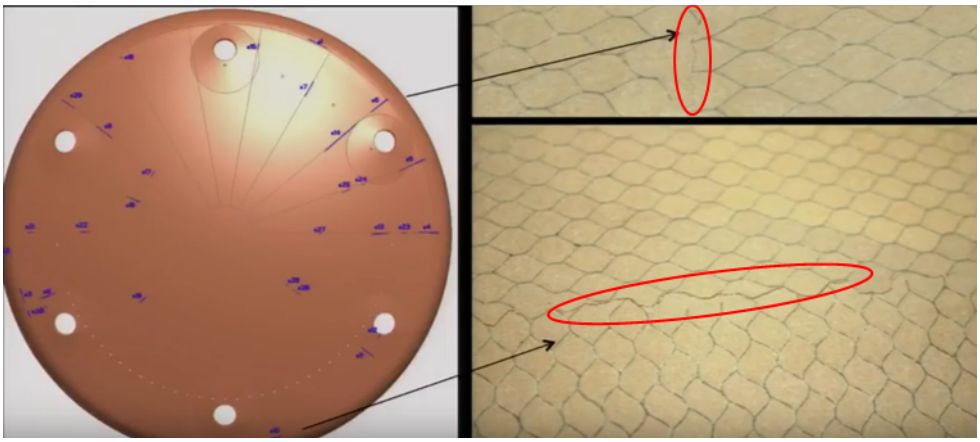

Figure 13. Typical EFT-1 Avcoat crack geometries[12]

The Apollo Program developed and implemented a repair process because Avcoat cracking was a known issue at the time. Indeed, all Apollo Command Module spacecraft had these repairs, as shown in Figure 14.

Figure 14. Apollo plug repair[12]

The issues associated with Avcoat cracking on Orion were corrected in the field using a repair process derived from original Apollo processes. While the repair process was recertified for the MPCV implementation, much of the heritage Apollo process remained intact.

The Orion Program conducted a root-cause analysis of these failures, but that analysis was inconclusive as to their source. Subsequently, the NASA Engineering and Safety Center embarked on a multi-year root cause analysis of both failures. It must be recognized that the Orion EFT-1 flight heatshield design was successful in completing its test flight using the repair procedure developed from the heritage Apollo design.

The over-reliance on the historical architecture without understanding how other parameters (e.g., underlying substructure, material changes, scale) can affect both the heat transfer and structural response of the combined substructure and ablator system, demonstrated an example of using blind trust in a heritage application.

The monolithic Apollo architecture was even recognized by the Apollo Program as having introduced technical and programmatic risks, but the Apollo experience was to move away from the block architecture of Mercury to the honeycomb design. The rationale at that time was that the honeycomb system provides a fail-safe design[9] compared to the block design, where loss of a single block could result in a catastrophic hazard.

Even with the fundamental thermal and structural differences, Orion probabilistic risk assessments[11]predicted a loss of vehicle risk of 1-in-160,000 of Avcoat cracking in flight due to the inherent fault tolerance of the honeycomb Avcoat design. The successful flight test of the EFT-1 vehicle showed the merits of this historical design. However, moving to the EM-1 design, the Orion Program determined that transitioning from the Apollo architecture and to a bonded block design would provide cost, schedule, weight, and technical performance benefits[10].

In this case of the "grass is greener" syndrome, the Orion Program assumed there would be tangible advantages, reversing the lessons learned from Mercury to Apollo, including

- Improved inspection with off-the-vehicle non-destructive evaluation (NDE) of fabricated blocks prior to attachment
- Improved acceptance criteria to reject low-strength blocks via acceptance testing
- No interface issues due to lack of seams
- Reduced schedule risk due to greater availability of the heat shield during the vehicle integration process flow
- Reduced cost due to less touch labor associated with individual filling of honeycomb cells

On the surface, the cost and schedule advantages could be rationale for change assuming the technical and flight safety risks were comparable between the architectures. By moving most fabrication off the vehicle and instead relying on the bonding of approximately 300 blocks, processing of the vehicle could be changed from a serial to a more parallel process. However, even though molded blocks are associated with lower manufacturing costs, they introduced additional work not originally anticipated.

Preliminary assessments used to rationalize the change in architecture did not account for unknown unknowns in the implementation. For example, new NDE techniques[10] had to be developed to reduce the risk of inadequate structural bonding between the blocks and structural substrate. Traditional NDE techniques were not capable of adequately detecting flaws due to the materials and geometric features, as shown in Figure 15. This new Terahertz inspection process proved to be a cost, schedule, and technical risk. The cost and schedule impacts were due to this being a new development taken on by the Orion Program when it was found the existing techniques were not suitable. The technical risk was associated with the use of materials during the NDE process that could have affected the flight performance of the Avcoat insulation blocks. Extensive testing was required to demonstrate that these NDE materials would not affect the ablative or mechanical performance of the Avcoat.

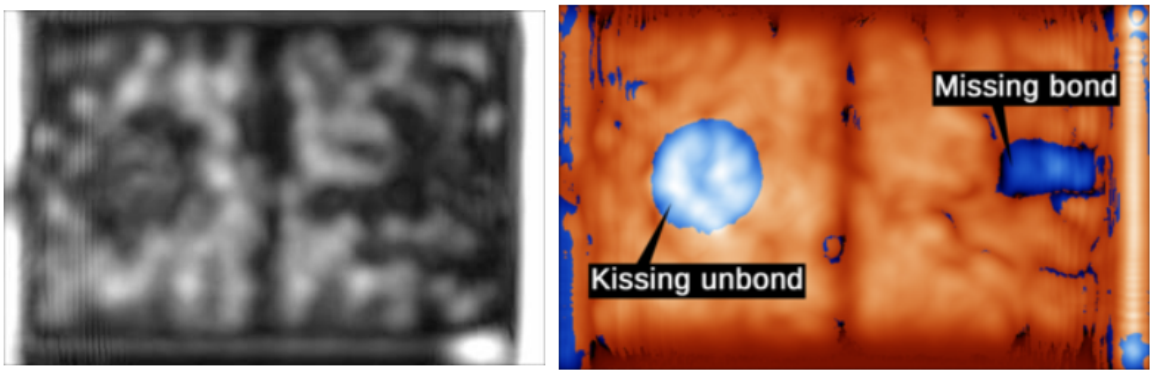

Figure 15. Improved NDE of Avcoat blocks[13]

Additionally, exhaustive test campaigns were conducted, due to the emergence of new failure modes associated with a block design that differed from the EFT-1 honeycomb architecture, namely crack propagation within Avcoat blocks or along bond line interfaces. A fracture-based approach has been targeted for heat shield certification to address some areas of structural integrity. The measurement of either within Avcoat fracture toughness or the toughness of adhesive bonds between Avcoat and the composite substrate has been a challenge, particularly at temperatures above the glass transition temperature of Avcoat.

Beyond the fracture testing currently being performed, significant efforts have been undertaken in the area of finite element analysis to assess the susceptibility to continued flaw growth due to undetected initial flaws either at adhesive bonds or within the material. This has led to development work for guidelines on how to discretize models, global-local methods to map data from the flight model to fracture models, and additional materials testing to validate models. These activities, which were not anticipated in the original decision to switch from the monolithic to block architecture, have impacted both the cost and schedule of the heat shield certification.

The "grass is greener" mentality was in full force in the decision to switch architectures from monolithic honeycomb to bonded blocks. The lessons learned by the Gemini and Apollo design teams were not followed. The technical team did not fully appreciate the differences in failure modes between a monolithic and block architecture, and how those failure modes could affect mission risk. These new design and certification challenges were not anticipated, and this has directly led to an increased amount of design certification to validate that the system has appropriate damage tolerance and flight safety.

The decision to change from the monolithic to block architecture was not taken lightly. Programmatically, there were perceived cost and schedule benefits to switching. Clearly, the manufacturing of blocks and subsequent manual bonding to the substrate is less labor intensive compared to manually injecting material into hundreds of thousands of cells, thus directly affecting both cost and schedule. Additionally, the block architecture releases the flight vehicle from flight processing flow constraints, providing flexibility of that integration flow. These are valid programmatic reasons for implementing a change, but the technical teams should have been more proactive in clearly outlining to program management the new schedule, cost, and technical challenges associated with an architecture change instead of optimistic projections. Whether or not

the "grass is greener" will only be understood after the Orion EM-1 and future missions are completed.

> *Lesson: Do not blindly trust historical architecture data before utilizing it for new designs, and do not move to newer architectures without fully understanding new failure modes that are introduced*

Lesson Learned #4: Inadequate Analyses May Still Give Answers; Perhaps Not Correct Ones (ISS Node Gusset Issue)

In preparation for launch of the first International Space Station (ISS) pressurized module, Node-1, high strains were observed in the radial port low-wall gussets[14]. Finite Element Analysis (FEA) had used Node-1 models with coarse 2D shell elements without running a mesh convergence check. These high strains were considered a modelling aberration that would improve once more detailed analysis was performed. It did not work out that way. In fact, the coarse elements had masked the strain gradients and true peaks in the region. The gussets had an E-beam weld area with low strength allowables, which made the situation worse. Figure 16 provides the gusset details.

A subsequent assembly level FEA of the Common Berthing Mechanism (CBM) utilized detailed Finite Element Models (FEM) of two pressurized elements on each side of the CBM and found an even higher strain peak in the gussets. The added stiffness in the assembly level FEA had made the problem worse. This finding put the Node-1 proof pressure campaign in jeopardy and presented safety and schedule risks to the first US element launch on STS-88. This issue became the focus of intense scrutiny by all stakeholders and the news media. A Blue Ribbon committee was formed with experts from Boeing, NASA, and the aerospace industry chartered to examine, review, advise, and suggest modifications and monitor progress towards a solution.

Preliminary investigations revealed the high gusset strains were the result of a pre-critical design review (CDR) mass-reduction campaign. The original Node-1 design had internal struts inter-connecting the four radial berthing ports to maintain Common Berthing Mechanism (CBM) deformations within the berthing allowable envelope. This design provided a stiffness balance when other pressurized elements were added to the ports. To save mass, these internal struts were eliminated. Global effects of the strut removal were not investigated thoroughly and the role of these struts in reducing the gusset strain was not realized.

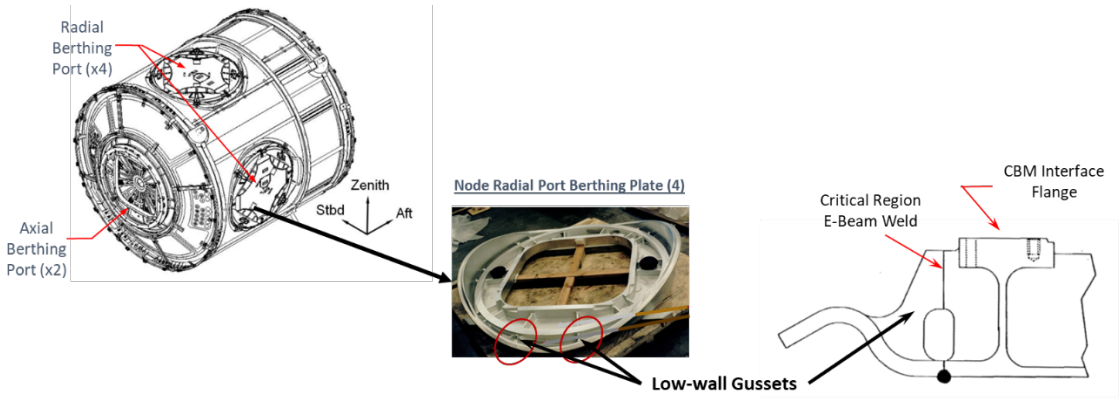

Figure 16. Radial Port Low-wall Gusset Details

Investigation

Detailed investigation campaign started with a study of the material properties. A coupon test campaign was launched at the Marshall Space Flight Center (MSFC) and the Langley Research Center (LaRC) test labs to generate as-built Al-2219 Electron-beam weld mechanical properties in order to ensure accuracy of the updated margins of safety. Additional mechanical testing was performed to assess stress creep behavior of the weld region. The gussets were loaded in the Short-Transverse (S-T) direction during Node pressurization, further exacerbating the problem because of the low ductility and percent strain-to-failure in that direction.

Detailed 2D Shell and 3D solid finite element models with optimized meshes (Figure 17) were developed to better understand gusset strains.

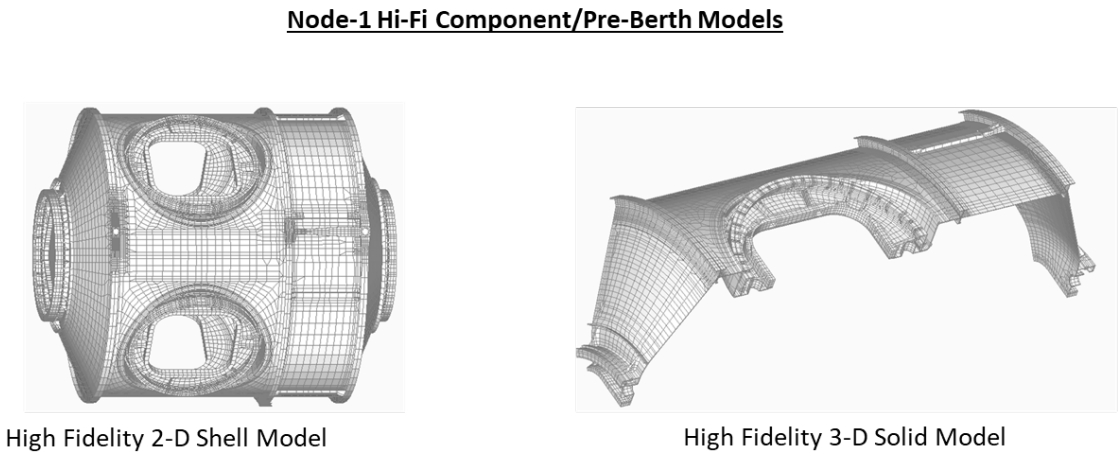

Figure 17. High Fidelity 2D and 3D Node Component Finite Element Models

A fully instrumented and outfitted Node Static Test Article (STA) was prepared for proof pressure testing (@22.5 psig) to validate the analysis predictions. Ten strategically located strain gages on each low-wall gusset provided real time strain measurements. Testing was halted prematurely at 20-psig when strains started a non-linear trend in low-wall gussets on each of the four radial ports, confirming model predictions. Strains continued to increase upon depressurization. A follow-on

proof pressure test was conducted on the Node-1 flight module with no internal secondary structure nor closeout pressure domes. This test was halted at 17-psig due to non-linear strain profiles, ellipsoidal deformation of the pressure shell, and post-test creep as seen on Node-STA. Refined analyses and full-scale testing proved the gusset issue was not an analytical aberration.

Solution

All Node-1 2D and 3D FE models were refined and correlated to the full-scale pressure test data. Twenty-five design solutions were proposed and each was analyzed via test-correlated FEA. Loading conditions included pre-berth (component level) and post-berthed (assembly level) loading with hatches open and closed (Figure 18). The new design solutions ranged from addition of external straps to re-installation of internal struts to off-load the gussets. Of the three final candidates, the most promising solution suggested eliminating the four low-wall gussets on each radial port and re-introduction of internal struts to stiffen the berthing plate and prevent excessive CBM and Hatch distortions.

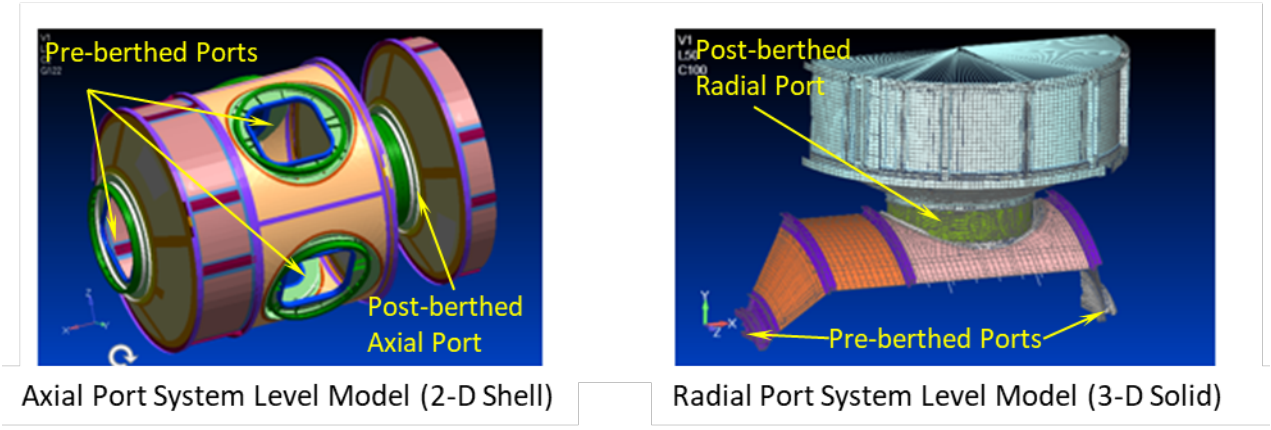

Figure 18. Hi –Fi System Level FEM (Pre-berth and post-berth configurations)

Removing the gussets posed a major concern. Node-STA and Node-1 gussets had experienced plastic strains during proof pressure test campaign. Removal of the gussets could relieve the berthing plate residual strains and result in four distorted berthing plates with the possibility of violating the CBM berthing envelope. Procedures were devised to measure residual strains and to systematically cut out the gussets with minimal distortion. Figure 19 highlights the gusset region before and after the modification.

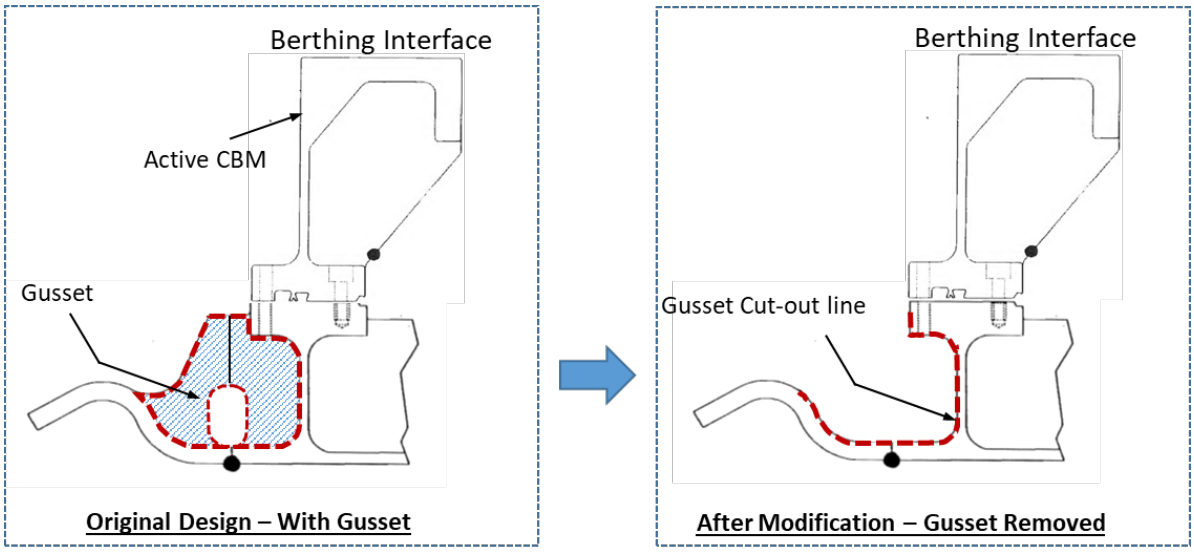

Figure 19. Radial Port Gusset before and after modification

Controlling the CBM and Hatch deflection with great precision is a key design requirement. Unfavorable distortions of the CBM flange at the Berthing Interface could potentially make the port unable to berth. It could impact the performance of automated berthing mechanisms, inability to seal the joint, compromise secondary internal seal installation, and negative structural margins of safety. Each deformation of the CBM ring, i.e., "ovality", Flange "surface flatness", out-of-plane "rotation", and tangential (clocking), must be within the prescribed envelope. Deformations are depicted in Figure 20.

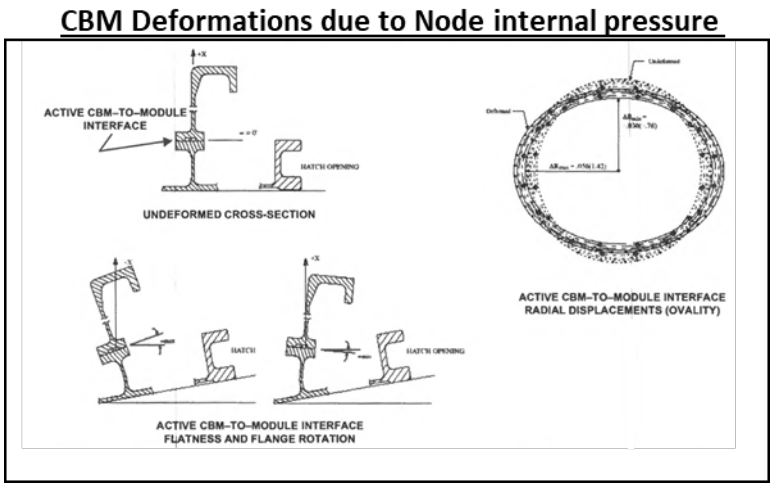

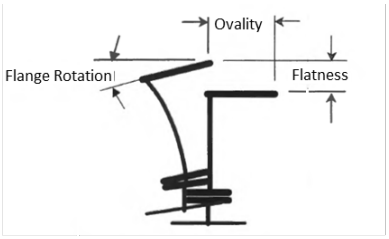

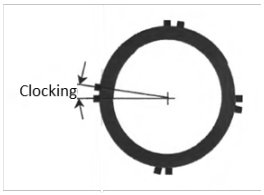

	Deformations			
	Ovality	Flatness	Flange Rotation	Clocking
Capture Dynamics	✓	✓	✓	✓
Powered Bolt/Nut Acquisition	✓	✓	✓	✓
Sealing (ACBM/PCBM)		✓	✓	
ICVA Seal (ACBM/PCBM)	✓	✓	✓	✓
Structural Strength	✓	✓	✓	
CBM Static Fit (Interchangability)	✓	✓	✓	✓

Figure 20. Berthing interface deformations and their affect

New internal strut design must provide the ability of tuning the berthing plate stiffness to ensure the deformations do not violate the berthing envelope. This was accomplished by the addition of preloading features on the struts and then loading each strut to a specific preload. Strain gages were added on each strut to monitor the load on-ground as well as on-orbit as needed. Resulting design configuration included four pairs of titanium trusses, which inter-connected all four radial ports inside the Node and were preloaded to help distribute pressure loads throughout the shell. Figure 21 shows a sketch of the internal strut configurations.

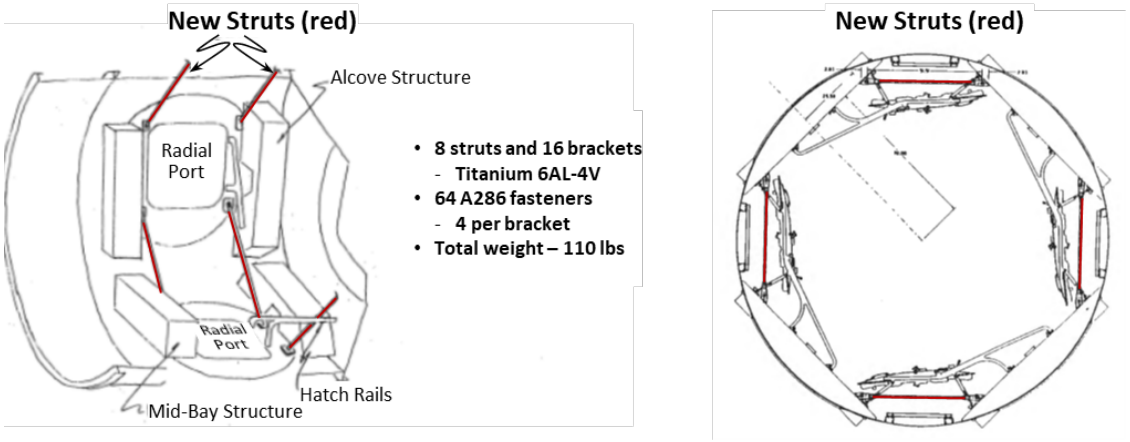

Figure 21. Node-1 Internal strut configuration

A summary of all the activities leading to final design modification is as follows:

1) Multiple high fidelity 2-D shell and 3-D solid Finite Element models created and correlated via full-scale proof test results.
2) Additional pressure tests on highly instrumented Node-STA and Node-1 performed to collect necessary data.
3) Coupon testing campaign to characterize gusset creep, residual strains, and elongation.
4) Machining approaches to cut the gussets with least structural impact due to weld and pressure induced residual stresses to minimize berthing flange distortions.
5) Hundreds of non-linear post-berthed assembly level analyses performed to characterize berthing plate response to stiffness changes affecting CBM berthing envelope.
6) Several internal strut design configurations to achieve the desired stiffness. Included strut design iterations, preload optimization/tuning calculations, and assembly planning.

With the modifications completed, Node-1 and Node-STA were successfully proof tested to the required 22.8-psig in pre-berth and post-berth CBM/vestibule configurations as well as with CBM bolt-out (fail-safe) configurations. (Note: For the Node-1 Proof Pressure Test, several major load-carrying pieces of internal secondary structure were included so that the overall deflection of the pressure shell would assume a similar cylindrical shape to the Node-1 STA). Test campaigns for the Node-STA continued and successfully achieved the combined pressure plus mechanical load conditions. To protect the proto-flight test article, the test factor of safety for the combined load was reduced to 1.05 x (pressure + mechanical) for an agreed upon conservative envelope of the specified transient dynamic interface loads on the radial ports. Node-1 was launched in December 1998 aboard STS-88 and has been operating flawlessly for over 21 years.

Lessons: 1) Poor meshing in Finite Element analyses can mask or hide underlying stress/strain profiles. Interpretation of FEA results requires due diligence. Do not ignore unfavorable results as a modeling aberration. 2)Any mass reduction campaign must include a thorough system level analysis to understand the local as well as global impact of stiffness changes.

CONCLUDING REMARKS

In this paper, four space flight assessments are presented and they each highlight important lessons to be learned. The first assessment recounted a substitution of metallic materials with another alloy to save weight, which on the face appeared to be inconsequential. While saving weight is every program manager's dream, before a substitution is implemented, a comprehensive analysis and evaluation of all aspects associated with the change needs to be performed to minimize unintended effects and avoid introduction of harmful consequences. The Al-2090 alloy selected as replacement material for External Tank stringers was a poor choice as it has low Short-Transverse (S-T) strength. Comprehensive analyses, testing and evaluation clearly demonstrated that the high stresses associated with fit-up and closing of gaps at the stringer feet produced cracks resulting from the low ST directional strength. The major lesson from this assessment is not to make design substitutions, especially to existing design configurations, without a comprehensive study of all aspects of the hardware configuration and loadings.

The second assessment outlined how combining worst-on-worst analyses from differing disciplines performed independently, may not be worst case when disciplines interact. In this case, separate thermal and mechanical analyses did not adequately capture the worst case of thermal-mechanical effects from a combined physics type analysis. Results from higher fidelity analyses may uncover design defects that were unanticipated or unaccounted for in the preliminary design/analysis process where traditional methods, using modified properties (knockdowns) and/or simplified assumptions are the norm. Hardware design/analysis cycles need to account correctly for multi-discipline environmental effects early in their development to reduce the possibility of significant design changes being required late in the process, when they tend to be much more expensive to -incorporate. The major lesson from this assessment is an understanding and correct simulation of all environments and their interactions in structural analysis is of utmost importance.

The third assessment outlines pitfalls of putting blind trust in performance of a historical architecture or design and then switching to a new hardware configuration, based on performance of the heritage design, and assuming that no new issues will arise due to the change. Fundamental differences existed between the heritage Apollo design and the Orion implementation, first using monolithic honeycomb approach and then changing to bonded blocks based on Avcoat material. The over-reliance on the historical architecture without understanding how other parameters (e.g., the underlying substructure, material changes, scale) could affect both the heat transfer and structural response of the combined substructure and ablator system demonstrated an example of using blind trust. A heritage design solution is no longer heritage if original assumptions or parameters are significantly changed.

The Orion Program determined that moving away from the Apollo architecture to a bonded block design would provide cost, schedule, weight, and technical performance benefits. On the surface, the cost and schedule advantages could be tangible rationale for change, assuming the technical and flight safety risks were comparable between the architectures. However, even though molded

blocks are associated with lower manufacturing costs, they introduced new failure modes and additional work not originally accounted for or anticipated. The "grass is greener" mentality could have influenced the decision to switch architectures and not follow the lessons learned by the Gemini and Apollo Programs.

The fourth assessment highlights the importance of Finite Element Modeling fidelity and the need for a comprehensive investigation of late-breaking design modifications. A mass-reduction campaign resulted in the removal of radial port internal struts on ISS Node-1 pressurized module. The verification analysis included only Node 1 component models with less than optimum mesh density. Observed localized strain peaks were discounted as modeling artifacts. Later, a system-level analysis with high fidelity (Hi-Fi) models revealed the strain peaks were real and even higher than originally predicted. Hi-Fi models included the CBM and pressurized element attached at the port, which added stiffness and drove the localized strain peaks at the radial port gussets. Struts had balanced the stiffness and helped unload the gussets. Resolution required a comprehensive test campaign, development of multiple higher fidelity 2-D shell and 3-D solid finite element models correlated to full-scale proof tests, a full set of system level models to predict all loading and stiffness scenarios, and structural modifications including return of internal struts. The lesson learned is, any FE model can give you an answer, but is it the right answer? Does the model have an optimized mesh density? Does it represent the assembled structure's stiffness? Are the loads and boundary conditions adequately understood and implemented?

References:

1. Knight, N. F., Song, K. C., Elliott, K. B, Warren, J. E., and Raju, I. S, "Space Transportation System (STS)133/External Tank (ET)-137 Intertank (IT) Foam Crack and Repair Assessment: Elastic-Plastic, Thermo-Mechanical Nonlinear Structural Analyses," NASA/TP-2012-217773, 2012.
2. Wingate, R. J., "Stress Analysis and Testing at the Marshall Space Flight Center to Study Cause and Corrective Action of Space Shuttle External Tank Stringer Failures," AIAA-2012-1776, 2012.
3. Phillips, D. R., Saxon, J. B., and Wingate, R. J., "Test-Analysis Correlation of the Single Stringer Bending Tests for the Space Shuttle ET-137 Intertank Stringer Crack Investigation," AIAA-2012-17.
4. Piascik, R. S., "Space transportation System (STS)-133/External Tank (ET)-137 Intertank (IT) Stringer Cracking Issue and Repair Assessment: Proximate Cause Determination and Material Characterization Study," NASA/TM-2011-217318. NESC-RP-10-00680, 2011.
5. Panda, J., Burnside, N. J., Fong, R. K., Ross, J. C., James, G. H., and Fogt, V. H., "Heated Helium to Simulate Surface Pressure Fluctuations Created by Rocket Motor Plumes," *AIAA Journal*, Vol 51, No. 2, 2013, pp. 302-314.
6. https://www.spaceflightinsider.com/missions/human-spaceflight/aerojet-rocketdynes-human-spaceflight-program-director-talks-orion/
7. Federal Aviation Administration, "Metallic Materials Properties Development and Standardization (MMPDS-04)," Chapter 2 – Steel Alloys, April 2008.

8. Hamm, K. R., Nee, X., Morr, D. E., Diaz-Aguado, M. F., "Thermo-Structural Analysis of 80-AS Wind Tunnel Model," NASA/TM-2019-220381, October 2019.
9. Pavlosky, J. E. and St Leger, L. G., "Apollo Experience Report: Thermal Protection Subsystem," NASA/TN-D-7564, 1974.
10. Koenig, W. J., Stewart, M., and Harris, R. F., "Orion Heat Shield Manufacturing Producibility Improvements for the EM-1 Flight Test Program," 39th IEEE Aerospace Conference 2018; 3-10 Mar. 2018; Big Sky, MT; United States, KSC-E-DAA-TN52588
11. Vander Kam, J., C. and Gage, P., "Estimating Orion Heat Shield Failure Due To Ablator Cracking During The EFT-1 Mission," NASA/ARC-E-DAA-TN31988, 2016
12. Vander Kam, J., "Burn to Shine: Experiences and Lessons from the Orion Heat Shield Lecture," https://www.youtube.com/watch?time_continue=442&v=ccJ6LpnSK20
13. "Bond Quality Inspection for Orion Heatshield Blocks," https://www.nasa.gov/feature/bond-quality-inspection-for-orion-heatshield-blocks
14. Zipay, J., Bernstein, K., Patin, R., Bruno, E., & Deloo, P., "Structural verification of the first orbital wonder of the world - the structural testing and analysis of the international space station (ISS)," AIAA 2012-1772.